Time-history and pushover analyses of asymmetric structures using a complex non-linear reinforced concrete model accounting for cracking.

Olivier Lherminier, Miquel Huguet, Boumediene Nedjar, Silvano Erlicher, Pierre Argoul

COMPDYN 2019
7th ECCOMAS Thematic Conference on
Computational Methods in Structural Dynamics and Earthquake Engineering
M. Papadrakakis, M. Fragiadakis (eds.)
Crete, Greece, 24-26 June 2019

TIME-HISTORY AND PUSHOVER ANALYSES OF ASYMMETRIC STRUCTURES USING AN EFFICIENT NON-LINEAR REINFORCED CONCRETE MODEL ACCOUNTING FOR CRACKING

LHERMINIER Olivier[1,2], HUGUET Miquel[2], NEDJAR Boumediene[1], ERLICHER Silvano[2], ARGOUL Pierre[1]

[1] IFSTTAR-MAST-EMGCU
14-20 Bd Newton, Cité Descartes, 77477 Marne-la-Valle Cedex 2
e-mail: olivier.lherminier@ifsttar.fr, pierre.argoul@ifsttar.fr, boumediene.nedjar@ifsttar.fr

[2] EGIS
4 rue Dolorès Ibarruri, 93188 Montreuil Cedex
e-mail: silvano.erlicher@egis.fr, miquel.huguet-aguilera@egis.fr

Keywords: Reinforced concrete, Cracking, Damage, Off-plane bending and shearing, Seismic margin assessment, Post-earthquake state, Non-linear constitutive model, Finite elements.

Abstract. *Non-linear calculation results can be significantly different when considering monotone or cyclic analyses. The crack opening and re-closing phenomena are quite difficult to represent with non-linear constitutive models using finite elements methods. The comparison between seismic time-history and pushover analyses is performed in this paper using GLRC_HEGIS non-linear global model for reinforced concrete mono-layer shell elements. It takes into account four different dissipative phenomena: concrete cracking, concrete damage, steel-concrete slip and steel yielding, by means of an analytical multi-scale analysis. This stress-resultant model is formulated for cyclic calculations in the framework of the thermodynamics of irreversible processes, in order to allow efficient numerical computations of earthquake engineering applications of RC buildings. This paper explores the validity range of this constitutive law through cyclic time-history analyses (that consider the crack opening and re-closing phenomena) and monotone pushover static analyses on asymmetric structures of CASH and SMART benchmarks. Pushover analysis is a nonlinear static procedure for evaluating the seismic margin of buildings accounting for their non-linear behavior. The pushover method used in this paper is the so-called Enhanced Direct Vectorial Addition (E-DVA) which defines the load pattern for the pushover analysis as a linear combination of load patterns proportional to the mode shapes. As this method is based on the application of a static force field with constant shape and increasing amplitude, only monotone non-linear phenomena are taken into account. The pushover and time-history analyses are performed (i) on the CASH benchmark model representing a multi-storey shear wall of a real nuclear power plant building structure and (ii) on the SMART benchmark mock-up representing a typical RC building of a nuclear facility. Several numerical comparisons are made at both global and Gauss points levels and are focused on the global mechanical behaviour and the computation of crack opening.*

1 Introduction

In many applications, RC structural analysis is usually realized by design offices using Finite Element (FE) models accounting for a structural linear elastic behaviour. However, in some cases (e.g. nuclear buildings), structural verifications have to be performed under extreme seismic solicitations; in this case, a non-linear behaviour is needed for RC cyclic calculations. Moreover, from a structural and earthquake-resistant point of view, when the bracing system of a structure essentially consists in shells connected to each other and to the slabs by heavily armed chaining, the contribution of RC slabs and walls have to be well represented.

The non-linear behaviour at the global scale of a RC element can be defined by the apparition and the evolution of different non-linear physical phenomena that dissipate energy. In this paper, the RC walls and slabs of the analyzed structures are modelled by GLRC_HEGIS [1] constitutive model. This thermodynamic admissible law accounts for four non-linear mechanisms: concrete cracking, concrete damage (or stiffness reduction), steel-concrete relative slip and steel yielding. It allows an efficient global modelling using a mono-layer shell FE, since the multiscale analysis has been performed analytically and the model implementation only accounts for the formulation at the global scale (macro-scale). A lot of information is available at the end of a FE calculation with GLRC_HEGIS since many results of interest (as crack width, steel plastic strain...) are internal variables of the model. More details about this constitutive model are presented in chapter 2.

In this paper, the seismic action is taken into account by two different methods: nonlinear time-history and nonlinear pseudo-static pushover analyses. The basic (or classical) version of the pushover method is based on three main assumptions: (i) the structure has a plane of symmetry; (ii) there is a single horizontal earthquake component, parallel to the plane of symmetry; (iii) the dynamic behavior is governed by a dominant mode of vibration (with high effective mass). Therefore, the basic pushover analysis cannot be applied for the assessment of global torsion, local effects or influence of high frequency modes, and asymmetric buildings cannot be analyzed. For that reason, in this paper the Enhanced Direct Vectorial Approach (E-DVA) [2] is used to take into account many modes of irregular buildings under a multi-component earthquake. The load pattern for the pushover analysis is defined as a linear combination of modal load patterns using the modal weighting factors (called α-factors), which are calculated using the elliptical response envelopes. The details of this pushover method are presented in chapter 3.

These two seismic nonlinear methods (time-history and pushover analysis) are compared with each other by application to two different structures in chapter 4. First, a four-story framed in-plane irregular asymmetric wall extracted from the CASH benchmark is analyzed in section 4.1. Then, the three-story RC building of SMART benchmark is considered in section 4.2, accounting for the nonlinear behavior of its RC walls and slabs. Comparisons are done at the global (force, displacements) and local (crack width, steel yielding...) scales to analyze the pertinence and the interest of each of these two different nonlinear methods for seismic structural analysis.

2 Constitutive model: GLRC_HEGIS law for RC walls and slabs

An efficient and realistic material cyclic constitutive model is necessary for the comparison between the different seismic calculation approaches. Since the applications in chapter 4 are RC structures composed by walls and slabs, the GLRC_HEGIS model [1] is used for the material modelling. As shown in [3], this model is adapted to nonlinear seismic applications.

The model is implemented in the FE software Code_Aster [4] and allows an efficient global modelling and computation since it is implemented in mono-layer shell FE, accounting for an equivalent "reinforced concrete material". In order to obtain a stress-resultant model accounting for many nonlinear cyclic local phenomena which are at the origin of the nonlinear global behavior of RC elements, an analytical multi-scale analysis has been performed in [1]. Therefore, there is no need of time-costly numerical multi-scale analysis at each Gauss point and at each load step. The resulting model is formulated in the framework of the Thermodynamics of Irreversible Processes; the detailed formulation can be found in [5]. The four different local nonlinear cyclic mechanisms taken into account by GLRC_HEGIS are the following ones:

- Concrete cracking is the development of concrete displacement discontinuities (or macro-cracks) caused by tensile stresses. At each Gauss point, a constant average stabilized crack pattern characterized by the crack spacing s_r (obtained with Vecchio and Collins [6] formula) and orientation θ_r (perpendicular to the principal tensile strength) appears when tensile forces reach the concrete tensile strength f_{ct}. After this cracking onset, these two parameters remain known and constant (fixed crack model), where only the normal (crack width) w_n and tangential w_t crack displacements evolve with the applied force by following the retained bridging stress and aggregate interlock local laws respectively. Four family of cracks are considered: for each layer (top and bottom) of the RC shells, the typical crack pattern of RC walls submitted to cyclic in-plane shear loading can be reproduced by two family of cracks characterized by two different crack orientations.

- Concrete damage is assumed to be associated with the onset and development of homogeneous diffuse micro-cracking, which results in a concrete stiffness reduction. This degradation of concrete stiffness only takes place at high strain levels, above the limit value in tension f_{ct}/E_c. Therefore, concrete damage is supposed to be associated to compressive concrete behaviour. GLRC_HEGIS considers concrete damage as isotropic and it is introduced as an internal damage variable d scalar (two values, defined for both top and bottom layers of the RC shell), positive, non-decreasing in time and which can evolve only at high stress states.

- Relative slip between concrete and steel bars originates bond stresses for each x and y and top and bottom steel reinforcement layers. As stresses are transmitted from steel to concrete between consecutive cracks, this phenomena is at the origin of the tension stiffening effect. GLRC_HEGIS model uses an inelastic steel-concrete slip variable to limit the average tension stiffening effect to values given by the codes like [7].

- Steel reinforcement yielding is supposed to be concentrated at the crack crossings due to the steel-concrete stress transfer by bond. GLRC_HEGIS model considers that reinforcement bars only carry longitudinal forces and that the constitutive law is elastic-perfectly plastic characterized by a constant threshold equal to the steel yielding stress f_{sy}.

3 Pushover method: the Enhanced Direct Vectorial Approach (E-DVA)

The pushover analysis is a seismic nonlinear calculation method based on the application of a static force field with constant pattern and increasing amplitude on a nonlinear structural model. In the basic versions, the pattern of the applied load is generally chosen as proportional to the deformed shape of the dominant vibration mode for a given earthquake component. Other conventional patterns are constant or triangular, or more complex when choosing the vector of the CQC (Complete Quadratic Combination) of the pseudo-accelerations for a given earthquake component. Some adaptive approaches exist, where the load pattern is updated to account for the effects of the non-linear phenomena.

As presented in section 1, the basic version of the pushover analysis does not reproduce accurately the seismic behavior of no-perfectly regular and no-perfectly symmetric structures. For that reason and for the numerical comparisons of this paper, more advanced pushover methods are needed in order to account for interesting and conclusive results. When doing a pushover analysis, the loading pattern selection is likely more critical than the accurate determination of the target displacement.

Several generalizations of the basic pushover analysis have been proposed in the past years, in particular by Chopra and co-workers [8, 9, 10, 11], Fajfar and co-workers [13, 12, 14] and Penelis and Papanikolaou [15]. Some of these approaches take into account the possible multi-modal structural behavior, but all assume that the earthquake is mono-component. The Direct Vectorial Addition (DVA) (Kunnath [16], Lopez-Menjivar [17]) extends the pushover method to the case of multi-component earthquake by application of a load pattern obtained by a linear combination on the modes and earthquake directions.

The E-DVA pushover method is used in this work. It is based on the DVA approach and a rigorous definition of the weighting factors (α-factors) is provided, based on the notion of response envelopes of Menun and Der Kiureghian ([18]). This definition for the load pattern was first proposed by Erlicher et al. [20], which allows imposing an a priori chosen response of the structure. The pertinence of this pushover approach when comparing to time-history non linear analysis has been shown in [21]-[22].

3.1 The load pattern as a linear combination of modes

On the global axes (x, y, z) of the FE model of a structure, the mass $\underline{\underline{M}}$ (assumed diagonal) and the stiffness matrix $\underline{\underline{K}}$ are defined. It is supposed that the seismic input may have 1, 2 or 3 translational components, whose corresponding ground accelerations are named $a_{g,x}(t)$, $a_{g,y}(t)$ and $a_{g,z}(t)$, which act in the directions given by the influence vectors $\underline{\Delta_k}$ corresponding to the translation in the $k = x, y, z$ direction.

The non-adaptative pushover analysis are defined by a nodal force vector $\underline{q}_{pushover}(t)$ with constant shape and increasing amplitude:

$$\underline{q}_{pushover}(t) = c(t)\underline{Q} \tag{1}$$

where $c(t)$ is a scalar increasing pseudo-time function and $\underline{Q}$ is the constant vector defining the pattern of the nodal force field (a displacement-driven is also equivalently possible). The E-DVA approach defines this load pattern as:

$$\underline{Q} = \sum_{k=1}^{n_{ec}} \sum_{i=1}^{n} \alpha_{i,k} \underline{\underline{M}} \cdot \underline{A}_{max,i,k} \tag{2}$$

where $\alpha_{max,i,k}$ is the linear combination factor and $\underline{A}_{max,i,k}$ is the maximum pseudo-acceleration vector for the for the n retained modes i and n_{ec} earthquake directions k:

$$\underline{A}_{max,i,k} = (2\pi f_i)^2 S_{d,k}(f_i, \xi_i)\gamma_{i,k}\underline{\Phi}_i \tag{3}$$

where $S_{d,k}(f,\xi)$ is the response spectrum, f_i ,ξ_i and $\underline{\Phi}_i$ are respectively the modal frequency, damping ratio and deformed shape of mode i, and $\gamma_{i,k}$ is the participation factor of mode i with respect to earthquake direction k.

3.2 Different pushover analyses for different load cases

It can be shown that any response vector any any time $\underline{f}(t)$ (vector containing forces and/or displacements and/or stresses...) can be written as a linear combination of modal responses with the weighting factors $\alpha_{i,k}(t)$ [20]. Actually, only some response vectors are of interest when comparing to time-history analyses, those that maximize the value of parameters of interest, e.g. that maximum force in the x direction at the basis of a building or the maximum displacement in the y direction of a point of the roof. These response vectors corresponding to the load cases that maximize the interest parameters can be obtained using the notion of elliptical responses, as done in [21].

Once the response vector $\underline{f}(t)$ is known, the vector of modal combination $\underline{\alpha}$ is calculated following Erlicher et al. [20]:

$$\underline{\alpha} = \underline{\underline{\tilde{H}}} \cdot \underline{\underline{R}}_f \cdot \underline{\underline{X}}_f^{-1} \cdot \underline{f} \tag{4}$$

where $\underline{\underline{\tilde{H}}}$ is the modal coefficient correlation matrix, $\underline{\underline{R}}_f$ is the modal response vector matrix and $\underline{\underline{X}}_f = \underline{\underline{R}}_f^T \cdot \underline{\underline{\tilde{H}}} \cdot \underline{\underline{R}}_f$ is the matrix which defines the elliptical domain of the concomitant values of $\underline{f}$ by:

$$\underline{f}^T \cdot \underline{\underline{X}}_f^{-1} \cdot \underline{f} \leq 1 \tag{5}$$

Finally, in Erlicher et al. [24] a method is proposed to choose several dominant modes to reach the searched response. As the total value of the response vector is $\underline{f} = \underline{\underline{R}}_f^T \cdot \underline{\alpha}$, the value of the parameter of interest of the response vector is compared to the cumulative contribution of each mode (and earthquake direction) by means of the sum of the products between α_{ik} and the corresponding line of $\underline{\underline{R}}_f$, for the column corresponding to the parameter of interest.

3.3 The equivalent seismic spectrum for multi-direction earthquakes

A difficulty exists when trying to define the response spectrum for an earthquake acting in the direction of the earthquake $\underline{t}$, which is identified as the direction of the resultant of the load pattern $\underline{Q}$. By considering the deformed shape $\underline{U}$ under $\underline{Q}$ load $\underline{U} = \underline{\underline{K}}^{-1} \cdot \underline{Q}$, the participation factor of $\underline{U}$ in the $\underline{t}$ direction can be defined. In this direction, the structure vibrates with an equivalent frequency f^* and damping ratio ξ^*.

For a single-component earthquake, the maximum displacement can be easily calculated from the corresponding spectrum. For example, for single-component earthquake in direction $k = x$, one has $\gamma_{U,t} = \gamma_{U,x}$ and the response spectrum is $S_{d,x}(f^*, \xi^*)$. Analogous formulas can be written for earthquake components y and z. Based on the assumption of non-correlation between accelerograms in the x, y and z directions, the SRSS combination is used to define s_{max} for a multi-component earthquake:

$$S_{d,t}(f^*, \xi^*) := \frac{1}{|\gamma_{U,t}|}\sqrt{(\gamma_{U,x}S_{d,x}(f^*,\xi^*))^2 + (\gamma_{U,y}S_{d,y}(f^*,\xi^*))^2 + (\gamma_{U,z}S_{d,z}(f^*,\xi^*))^2} \tag{6}$$

4 Numerical Applications

4.1 Irregular wall from CASH : Benchmark on the beyond design seismic capacity of reinforced concrete shear walls

CASH is an international benchmark organised by the OEDC-NEA (Nuclear Energy Agency). The main purpose is to evaluate the accuracy of tools and prediction methods used in civil engineering for the estimation of the seismic capacity of shear reinforced concrete walls in "beyond design" seismic situation (important seismic excitation). The benchmark study focuses on two different multi-storey shear walls representative of a real NPP building structure. The results presented in the article are those obtained for the irregular structure (Figure 1-b) and the following post-treatment results are not those presented to the benchmark but are only examined for the purpose this article.

4.1.1 Model description

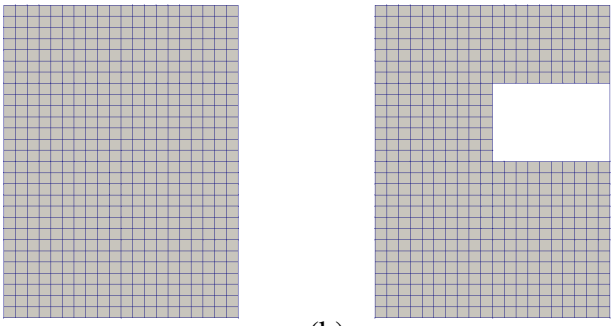

(a) (b)

Figure 1: CASH Finite Element models on Code_Aster

The structure represents the facade of a building with four floors, the studies are done in the plane (2D) of the wall. The height of the structure is 16m for 12m width and 0.40m thick. Slabs and out-of-plane walls are represented by beams and columns with strong depths. In-plane walls are modelled with shell elements using the GLRC_HEGIS global constitutive law and beams and columns are modelled with multifiber beams elements using the MAZARS constitutive law [23] for concrete fibers and an elastic-plastic model (with kinematic hardening) for steel fibers.

4.1.2 Modal and spectral analyses

The purpose of this section is to evaluate the linear response of the considered irregular structure for a given pseudo-acceleration spectrum. First, the modal analysis is performed and the corresponding spectral values are calculated.

The results of the modal analysis performed on the FE model are summarized in Table 1. The 5 retained modes account for 99% of the total mass for x and z directions.

4.1.3 Pushover analysis

The objective of this analysis is to evaluate the non-linear response of the wall under an increasing horizontal load proportional to a specific profile. The E-DVA method procedure described in [24] is applied step by step.

Modes	**Frequency [Hz]**	**Effective mass in X [kg]**	**Effective mass in Z [kg]**	$S_{a,X}$ $[m/s^2]$	**Damping factor [%]**
1	4.21	1730	0	4.06	2.00
2	14.1	422.0	0	2.37	1.36
3	24.1	0	21.80	1.91	1.54
4	24.8	0	373.0	1.79	1.75
5	26.2	68.80	0	1.71	1.95

Table 1: Five first modes calculated for the irregular CASH specimen

(a) Based on the modal basis above, response-spectrum analysis and CQC coefficients are used to determine the response matrix of the six efforts $\underline{f} = [F_x, F_y, F_z, M_{xx}, M_{yy}, M_{zz}]^T$ at the basis of the structure, for the spectra of Figure 1(c):

(b) The response matrix $\underline{\underline{X}}_f$ of Eq.(5) defining the ellipse of the maximum seismic efforts F_x, F_z is obtained from the first and the third rows and columns of the matrix.

(c) The choice of the loading direction is done here in the plan X-Z in the directions of the global coordinate system +X and -X to maximize the global forces $+F_x$ and $-F_x$.

(d) The corresponding $\underline{\alpha}$-vectors are computed using Eq. (4)

Direction	**+Fx**	**-Fx**
F_X (kN)	7571	-7571
f^* (Hz)	4.92	4.92
$\xi^*(\%)$	2.0	2.0
$\gamma_{U,X}(m^{-1})$	237	237
$[\underline{U}]_{j,X}$ (mm)	5.42	-5.42
	0.00	0.00
	-0.550	0.550

Table 2: Equivalent SDOF parameters for the considered load cases

Direction	**+Fx**		**-Fx**	
	Modes	Contribution	Modes	Contribution
	1	(90.4%)	1	(90.4%)
	2	(9.25%)	2	(9.25%)
	4	(0.302%)	4	(0.302%)
	3	(0.0%)	3	(0.0%)
	5	(0.0%)	5	(0.0%)
$\tilde{ik}_{max}$	1 mode is sufficient		1 mode is sufficient	

Table 3: Number of modes and corresponding percentage of the total response needed

(e) The procedure is applied to determine the dominant modes: based on the $\alpha_{i,k}$ factors calculated at step (d),the products $\alpha_{i,X}\underline{F}_{i,X}^T$ are computed for the two load cases. The cumulative sum of the products according to the order defined in Table 3 is normalized according

to the maximum response (second row of Table 2). For instance, when taking $C_d = 0.90$ as suggested in [25] at chapter 4.3.1(b), the first ik_{max} modes are dominant since their contribution to the response $F = \underline{f}^T \cdot \underline{b}$ is 90% of the total response. Table 3 shows that only the first mode is needed to fulfill this condition.

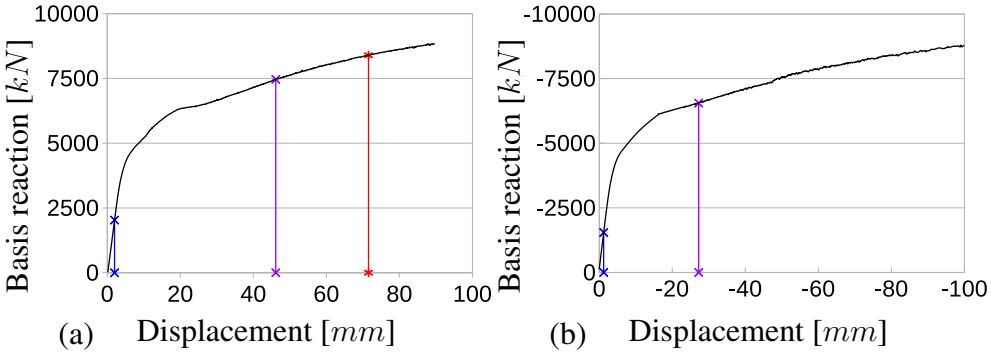

Figure 2: Pushover curve (Force-Displacement) for (a) +Fx and (b) -Fx load cases

The application of incremental unidirectional loading for pushover analysis gives global force-displacement curves which can be analyzed to distinguish the evolution of the activated non-linear phenomena. First, in Figure 2, a linear segment describe the non-cracked phase (before the blue line), then there is creation of several cracks. When the crack pattern is stabilized, the crack width increase and the steel reinforcement can yield (purple line) and finally a "tension-stiffening" effect can be observed. As shown in Figure 2, the concrete ultimate limit in compression is reached for a displacement of +72 mm (red line) and corresponds to a strain level of $\epsilon_u = 3.5‰$. It can be explained by the fact that the concrete developed too many micro-cracks in compression and can't bear more stress. The structure only reach its ultimate capacity in compression in the direction +Fx.

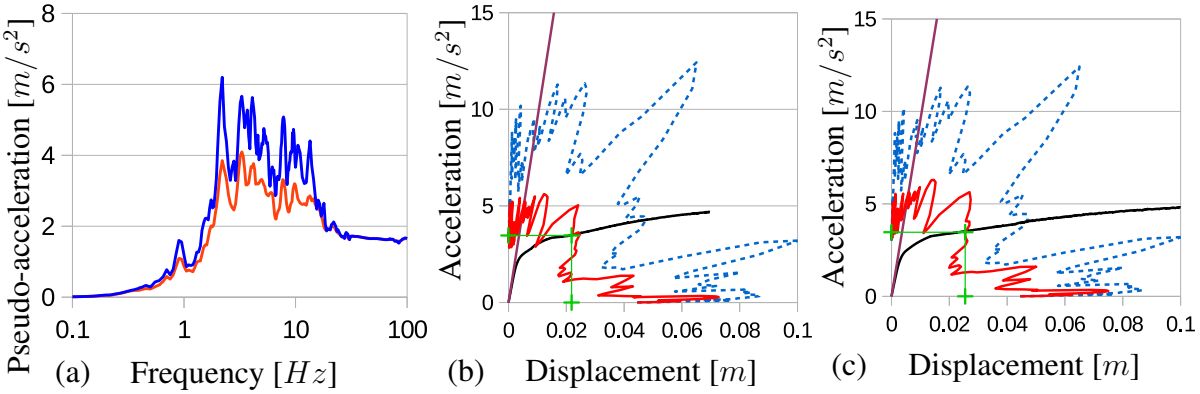

Figure 3: (a) Spectra and graphical results in the ADRS plane for the cases (b) +Fx (c) -Fx

Then, the coordinates of each target point are determined at the intersection of the capacity spectrum with the Acceleration Displacement Response Spectrum (ADRS) given by Eq. (6). The damping ratio $\tilde{\xi}^*$ of ADRS after iteration accounts for the hysteretic damping (Figure 3). The target point coordinates are shown in Table 4, with F_X and V_X corresponding to the obtained target global reaction and displacement of the structure, respectively.

Direction	+Fx	-Fx
$S_a(m/s^2)$	2.78	2.81
$S_d(mm)$	7.79	8.08
$\tilde{\xi}^*(\%)$	12.6	8.80
F_x(kN)	5257	-5272
V_x(mm)	10.18	-10.25

Table 4: Obtained target points for the considered load cases

4.1.4 Time history analysis

To evaluate the non-linear response of the irregular specimen under a horizontal seismic loading, a accelerogram whose spectrum corresponds to the one used in the pushover analysis is imposed to the structure. The chosen seismic input data is scaled to a $PGA = 0.16g$ intensity earthquake.

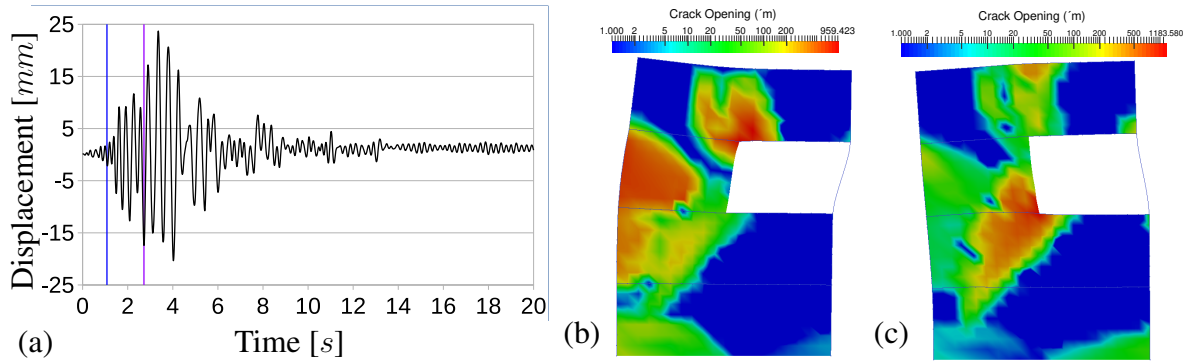

Figure 4: (a) Time-history roof displacement and obtained crack opening at (b) maximal displacement +Vx and (c) maximal displacement -Vx

The graphical results are shown in Figure 4 (a). Two non-linear indicators are given : the first concrete crack (blue line) and the first steel reinforcement yielding (purple line). The crack pattern at the maximal displacements in both directions are shown in Figure 4 (b) and (c).

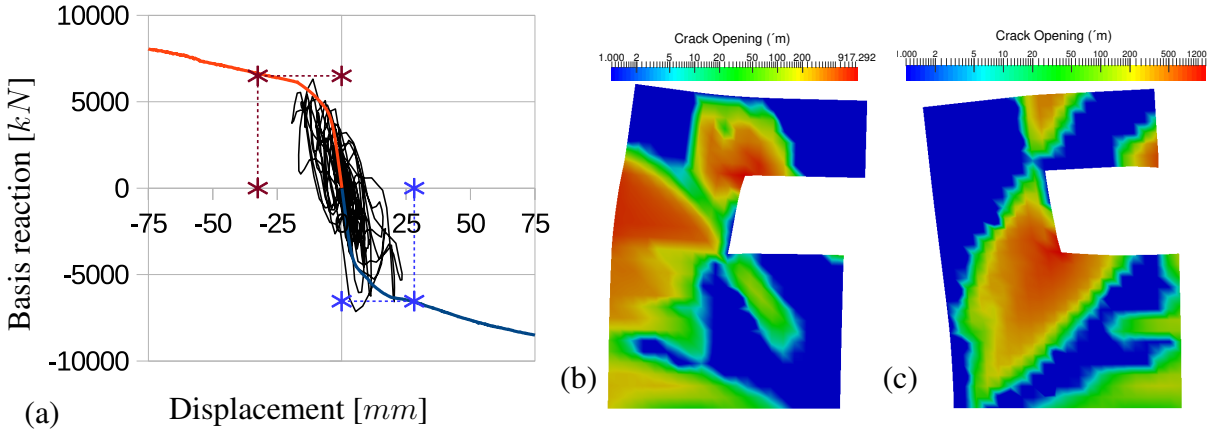

Figure 5: (a) Comparison of the capacity curves and obtained crack opening during the pushover analyses at (b) target point +Vx and (c) target point -Vx

4.1.5 Comparison between time history and pushover analyses

The graphical comparison of Figure 5 (a) shows that the dynamic results (black lines) are mostly inside the envelope area defined by the obtained target points (red and blue) and that the calculated forces that are presented in Table 4 are well estimated by the pushover (Figure 5 (a)) compared to the time-history results. The pushover results given by the E-DVA approach provide a suitable and accurate envelope of the maximum roof displacements and global forces at the basis of the building.

In order to compare the obtained crack pattern, the crack opening values using GLRC_HEGIS are plotted at the pushover target point. The results of Figure 5 (b) and (c) show that the crack patterns obtained by the pushover analyses are very close of the one obtained by time-history analysis showed in Figure 4 (b) and (c).

4.2 SMART: Seismic design and best-estimate Methods Assessment for Reinforced concrete buildings subjected to Torsion and non-linear effects

The experimental program SMART [26] was supported by the French companies Commissariat l′Energie Atomique et aux Energies Alternatives (CEA) and Electricite de France (EDF) and partially by the International Atomic Energy Agency (IAEA). The goals of the benchmark are to compare and to validate the used methods to evaluate the seismic responses of reinforced concrete structures under a seismic loading that induce 3D effects such as torsion and out-of-plane shear and to check the accuracy of prediction approaches of advanced calculation methods used in earthquake engineering.

4.2.1 Model description

The program concerns a $1/4$ scale mock-up of a representative asymmetric RC multi-storey building in nuclear power plants. The experimental moke-up was tested under seismic loadings applied by the shaking table with 6 degrees of freedom AZALE at CEA Saclay. The tested structure corresponds to SMART 2013 international benchmarks [26], but the foundation conditions are not respected in this article and all the comparisons to experimental results are out-of-scope of this paper. The structure shown in Figure 6(a) represents a asymmetric 3 storey reinforced

(a) 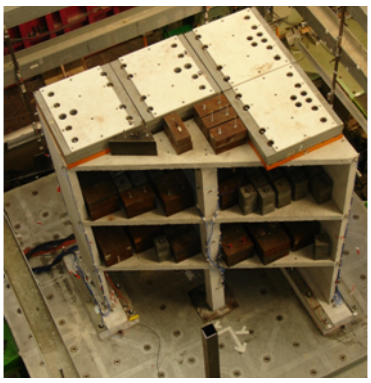 (b) 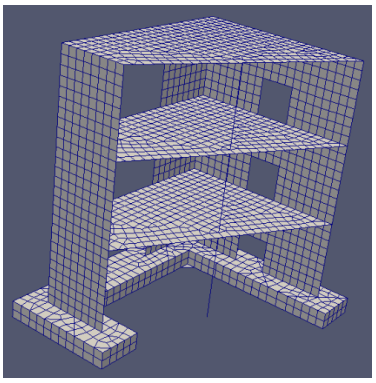

Figure 6: SMART (a) experimental moke-up and (b) used FE model on Code_Aster

concrete building and consists of RC slabs, walls, beams and columns. In the FE model of Figure 6(b), only the two first types of structural elements are modelled with the developed GLRC_HEGIS constitutive model, while beams and columns are modelled with a linear elastic

law. Therefore, all the non-linearities are originated by the nonlinear response of the developed model. The full building is 3.650 m height for 3.100 m width, walls are 10 cm thick and beams and columns are 15 cm and 20 cm thick respectively. In order to check the performances of the constitutive law GLRC_HEGIS, several studies were carried in parallel of the benchmark to compare the obtained results in the same way than those of the previous numerical application. Therefore, the shaking table was not taken into account here to save computation time but the benchmark will be fully conducted in a second time and the shaking table will be added.

For preliminary studies carried on the SMART building, several sets of seismic input data were generated. There particularity is that they all were generated from a unique aimed spectrum. Therefore, spectral, pushover and time-history results can be compared between each seismic input sets. The obtained pseudo-acceleration spectra were compared to only keep those which don't exceed a 10% error from the aimed spectrum, see Figure 7. All the generated accelerograms are different but the modes of the structure can be excited in a comparable way. The seismic intensity of the aimed spectrum is given by PGA$= 2.45m/s^2$.

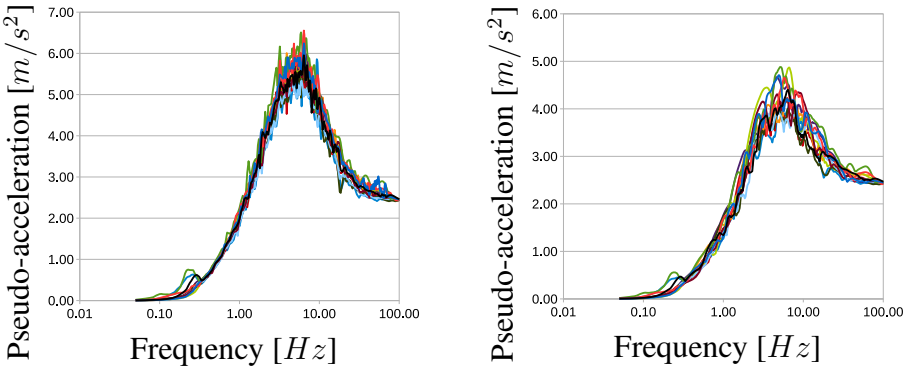

(a) Spectra at 5% damping

(b) Spectra at 10% damping

Figure 7: Chosen spectra associated to the seismic pseudo-acceleration inputs for the preliminary SMART studies

4.2.2 Modal and spectral analyses

First, the modal analysis is performed and the corresponding spectral values are calculated. The nine first modes are calculated for the structure. The results of the modal analysis performed on the FE model are summarized in Table 5. The 9 retained modes account for 83% of the total mass for x and y directions. The presented pushover method allows to choose along these modes which really need to be considered.

4.2.3 Pushover analysis

The E-DVA method procedure previously applied in section 4.1.3 is also applied to this 3D structure. The pushover directions are chosen here following 8 horizontal directions given by the Newmark combinations, as explained in [2].

Then, the coordinates of each target point are determined at the intersection of the capacity spectrum with the ADRS spectrum given by Eq. (6). The damping ratio $\tilde{\xi}^*$ of ADRS spectra

Modes	**Frequency [Hz]**	**Effective mass in X [%]**	**Effective mass in Y [%]**	$S_{a,X}$ $[m/s^2]$	$S_{a,Y}$ $[m/s^2]$	**Damping factor [%]**
1	8.47	52.6	8.19	6.77	6.77	2.81
2	15.2	15.9	52.8	6.41	5.80	2.97
3	29.8	13.2	7.48	3.78	4.10	4.49
4	30.8	0.53	2.19	3.58	4.06	4.60
5	32.5	0.05	0.39	3.45	4.04	4.81
6	32.7	0.00	1.58	3.42	4.01	4.84
7	35.5	0.56	0.46	2.79	3.74	5.17
8	35.6	1.63	1.08	2.74	3.75	5.19
9	37.1	0.31	0.00	2.57	3.86	5.37

Table 5: Nine first modes of the SMART FE model

θ	$12.9°$	$51.9°$	$122°$	$168°$
F_θ (kN)	222	197	198	225
F_x (kN)	216	121	106	-219
F_y (kN)	49.6	155	-167	48.6
f^* (Hz)	9.06	12.3	9.32	8.79
$\xi^*(\%)$	2.94	3.39	3.45	3.05
$\gamma_{U,t}(m^{-1})$	496.1	1044	560.5	453.3
	2.01	0.919	1.30	-2.20
$[\underline{U}]_{j,t}$ (mm)	-0.548	0.210	-1.05	0.959
	-0.059	0.001	-0.080	0.086

Table 6: Equivalent SDOF parameters for the considered load cases

$12.9°$		$51.9°$		$122°$		$168°$	
Modes		Modes		Modes		Modes	
1	(54.1%)	2	(87.5%)	2	(22.9%)	1	(78.7%)
2	(37.9%)	1	(5.97%)	1	(54.0%)	2	(5.93%)
3	(5.68%)	10	(4.83%)	3	(14.4%)	3	(12.4%)
10	(1.45%)	6	(0.794%)	10	(3.22%)	8	(1.08%)
8	(0.399%)	4	(0.519%)	4	(2.22%)	10	(0.492%)
4 modes are sufficient		4 modes are sufficient		7 modes are sufficient		6 modes are sufficient	

Table 7: Number of modes and corresponding percentage of the total response needed

after iteration accounts for the hysteretic damping (Figure 8). The target point coordinates are shown in Table 8, with F_t and V_t corresponding to the obtained target global reaction and displacement of the structure in the considered direction t.

4.2.4 Time history analysis

To evaluate the non-linear response of the irregular specimen under a horizontal seismic loading, accelerograms whose spectra correspond to those of Figure 7 used in the pushover analysis are imposed to the structure. The seismic input data are all scaled to a $PGA = 2.45m/s^2$ intensity earthquake. For the sake of brevity, only two time-history results are showed here.

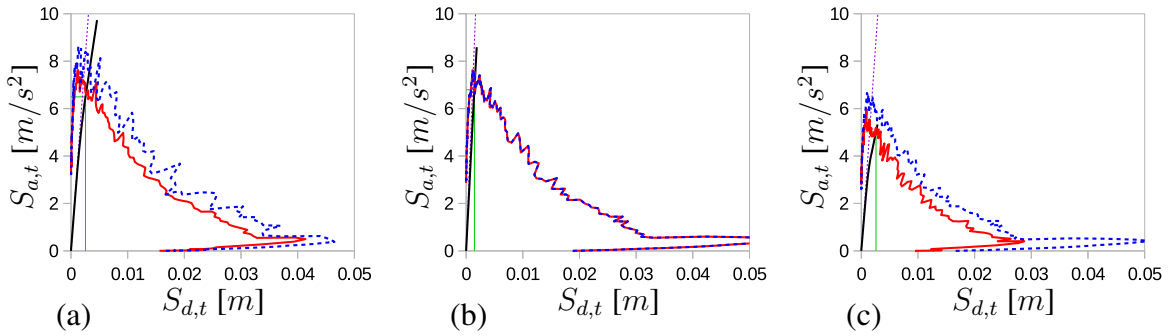

Figure 8: Capacity curves vs. spectrum in the ADRS plane for three of the load cases

Direction	12.9°	51.9°	122°	168°	−167°	−128°	−57.6°	−12.5°
$S_a(m/s^2)$	6.50	6.80	5.02	5.26	6.84	6.68	5.69	6.06
$S_d(mm)$	0.256	0.146	0.260	0.211	0.273	0.149	0.215	0.267
F_t(kN)	357	395	428	374	359	383	410	363
V_t(mm)	8.14	7.92	7.89	8.03	8.38	8.02	8.34	8.08
$\tilde{\xi}^*(\%)$	3.37	3.39	7.11	2.41	3.56	3.39	4.12	4.33

Table 8: Obtained target points for the considered load cases

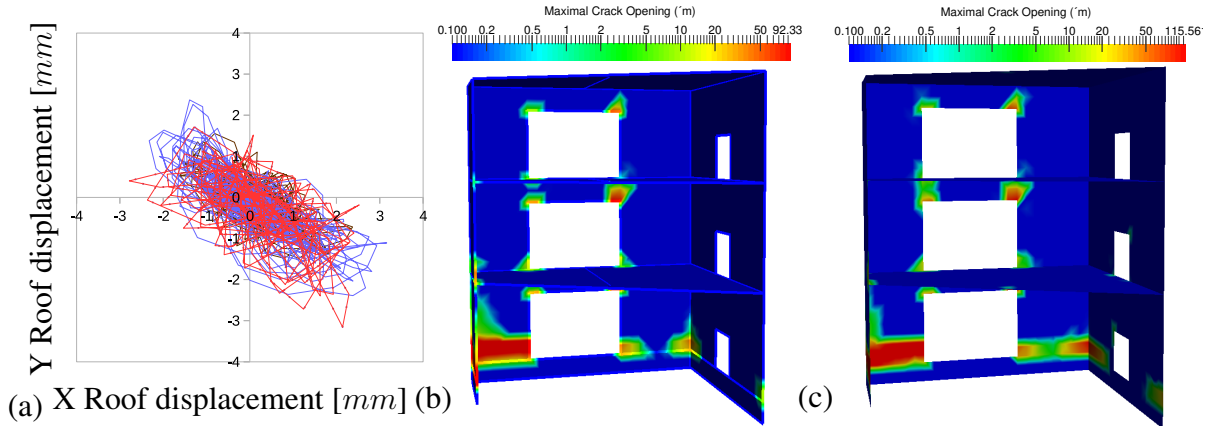

Figure 9: (a) Time-history roof displacement and maximal obtained crack opening during (b) a first seismic input and (c) a second one

The roof displacements shown in Figure 9 (a) are characteristic of an asymmetric structure with a dominant torsion mode. In Figures 9 (b) and (c), the maximal values of the crack opening during two whole earthquakes are plotted and represent the obtained crack patterns. When analyzing the results, it can be observed that the cracks are localized near the openings. The structure is heavily cracked at its left basis corner and steel reinforcement yielded.

4.2.5 Comparison between time history and pushover analyses

In order to compare the obtain results, the pushover results are plotted at their target point steps. The graphical comparison of Figure 10-a shows that the dynamic results obtained by all performed time-history analyses are mostly inside the envelope area defined by the obtained target points. The results show that the calculated forces that are presented in Table 7 are well

estimated (Figure 10-a). The pushover results given by the E-DVA approach provide a suitable and accurate envelope of the maximal global forces at the basis of the building.

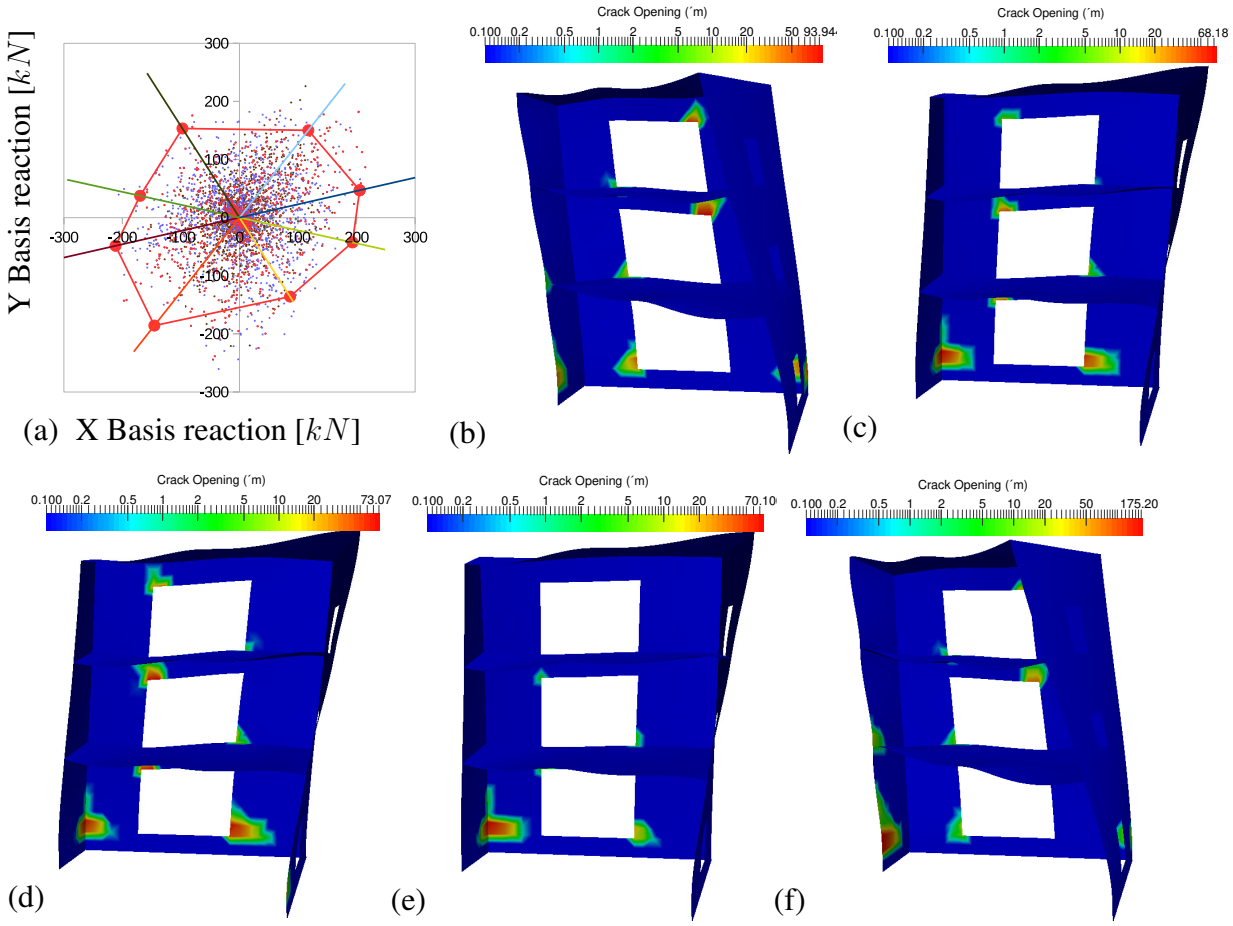

Figure 10: (a) Comparison of the capacity curves and obtained crack opening during the pushover analyses at (b) target point $12.9°$, (c) target point $168°$, (d) target point $-167°$, (e) target point $-57.6°$ and (f) target point $-12.5°$

The crack patterns obtained the pushover analyses (Figure 10-b-c-d-e-f) show that the crack opening are well estimated near the openings compared to the two time history crack opening pattern showed in Figure 9-b-c. As the time history analysis is a cyclic loading, the phenomena of cracking and reclosing cannot be reproduced by monotonic pushovers therefore several pushovers are needed to reproduce the crack pattern. The maximum obtained crack opening values obtained with the pushover analyses (Figures 10) give a quite accurate localization and value of the maximal crack opening obtained by time-history analyses (Figures 9). However, the severally cracked left basis corner due to the torsion behaviour of the structure cannot be fully predicted by pushover analyses that maximize basis reactions but it can be interesting in another study to perform multi-modal and multi-component pushover analyses that maximize the torsion (global torsion moment of the building M_{zz}).

5 Conclusions

The GLRC_HEGIS [1] model for RC plates (walls and slabs) is implemented for shell finite elements in Code_Aster [4] software and is applied to incremental static pushover and transient dynamic structural analyses corresponding to the same seismic intensity level. The structures which have been studied in this paper consisting of RC walls and slabs and the possibilities offered by this thermodynamic admissible law accounting for non-linear mechanisms have been used to compare available crack patterns at the end of a FE calculation since many results of interest (as crack width, steel plastic strain...) are internal variables of the with GLRC_HEGIS constitutive model.

In this paper, the seismic action has been taken into account by two different methods: non-linear time-history and nonlinear pseudo-static pushover analysis. In this paper the Enhanced Direct Vectorial Approach (E-DVA) [2] is used to take into account many modes of irregular buildings under a multi-component earthquake. The load pattern for the pushover analysis has been defined as a linear combination of modal load patterns using the modal weighting factors (called α-factors), which have been calculated using the elliptical response envelopes. The results obtained by time-history and pushover analyses have been compared.

First, a four-story framed in-plane irregular asymmetric wall extracted from the CASH benchmark has been analyzed in section 4.1. Then, the three-story RC building of SMART benchmark has been considered in section 4.2, accounting for the nonlinear behavior of its RC walls and slabs. Comparison between obtained results shows a relatively good fitting both at the local (e.g. crack width) and global (structural behavior) scales. The capabilities of the model to show the evolution of variables (crack width, steel reinforcement plastic strain, energy dissipation...) fields at every load step, and to estimate in a relatively accurate manner the RC section strength, have been also demonstrated. Comparisons have shown that forces and displacements can be estimated by pushover analyses and that time-history analyses have given a lot of local results (crack width, steel yielding...) that show the interest of each of these two different nonlinear methods for seismic structural analysis.

REFERENCES

[1] M. Huguet, S. Erlicher, P. Kotronis, F. Voldoire, Stress resultant nonlinear constitutive model for cracked reinforced concrete panels. *Engineering Fracture Mechanics*, **176**, 375–405, 2017.

[2] O. Lherminier, S. Erlicher and M. Huguet, Multi-modal pushover analysis for a multi-component earthquake: an operative method inspired by the Direct Vectorial Approach, *Proceedings of the 16th European Conference on Earthquake Engineering*, Thessaloniki, Greece, 2018.

[3] M. Huguet, M. Bourahla, S. Erlicher, P. Kotronis, GLRC_HEGIS global constitutive model for RC walls and slabs for seismic nonlinear structural analyses, *Proceedings of the 16th European Conference on Earthquake Engineering*, Thessaloniki, Greece, 2018.

[4] Electricité de France, Open source on www.code-aster.org. Finite element $Code\_Aster$, *Analysis of Structures and Thermomechanics for Studies and Research*, 1989–2017.

[5] M. Huguet, A homogenized nonlinear stress resultant constitutive model for cracked reinforced concrete panels *Ph.D. Thesis Report, Ecole Centrale Nantes / Egis*, 2016.

[6] F.J. Vecchio, M.P. Collins, The modified compression-field theory for reinforced concrete elements subjected to shear, *ACI Journal* **83:2**, 219–231, 1986.

[7] Comité Européen de Normalisation, *EuroCode 2 - 2004 Design of concrete structures: Part 1-1*, 2005.

[8] A.K. Chopra, R.K. Goel, Capacity-demand-diagram methods based on inelastic design spectrum, *Earthquake Spectra*, **15:4**, 1999.

[9] A.K. Chopra, R.K. Goel, A modal pushover analysis procedure for estimating seismic demands for buildings, *Earthquake Engineering and Structural Dynamics*, **31**, 561–582, 2002.

[10] A.K. Chopra, R.K. Goel, A modal pushover analysis procedure to estimate seismic demands for unsymmetric-plan buildings, *Earthquake Engineering & Structural Dynamics*, **33**, 903–927, 2004.

[11] R.K. Goel, A.K. Chopra, Evaluation of modal and FEMA pushover analyses: SAC buildings, *Earthquake Spectra*, **20:1**, 225–254, 2004.

[12] P. Fajfar, D. Marusic and I. Perus, The extension of the N2 method to asymmetric buildings, *Symposium on Earthquake Engineering Challenges and Trends, honoring Prof. Luis Esteva, J. J. Prez-Gaviln (Ed.)*, Univ. Nacional Aut. Mexico, ISBN: 970-32-3699-5, 2006.

[13] P. Faifar, A nonlinear analysis method for performance-based seismic design, *Earthquake Spectra*, **16:3**, 573–592, 2000.

[14] P. Fajfar, D. Marusic and I. Perus, Torsional effects in the pushover-based seismic analysis of buildings, *Journal of Earthquake Engineering*, **9:6**, 831–854, 2008.

[15] G.G. Penelis and V.K. Papanikolaou, Nonlinear static and dynamic behavior of a 16-story torsionally sensitive building designed according to Eurocodes, *Journal of Earthquake Engineering*, **14**, 706–725, 2010.

[16] S.K. Kunnath, Identification of modal combination for nonlinear static analysis of building structures, *Computer-Aided Civil and Infrastructure Engineering*, **19**, 246–259, 2004.

[17] M.A. Lopez-Menjivar, Verification of a displacement based adaptive pushover method for assessment of 2-D reinforced concrete buildings, PhD Thesis, European School for Advanced Studies in Reduction of Seismic Risk (ROSE School), University of Pavia, Italy, 2004.

[18] C. Menun and A. Der Kiureghian, Envelopes for seismic response vectors. I: Theory, *Journal of Structural Engineering*, **126:4**, 467–473, 2000.

[19] B. Gupta and S.K. Kunnath, Adaptive spectra-based pushover procedure for seismic evaluation of structures, *Earthquake Spectra*, **16:2**, 367–392, 2000.

[20] S. Erlicher, Q.S. Nguyen and F. Martin, Seismic design by the response spectrum method: a new interpretation of elliptical response envelopes and a novel equivalent static method based on probable linear combinations of modes, *Nuclear Engineering and Design*, **276**, 277–294, 2014.

[21] S. Erlicher and M. Huguet, A new approach for multi-modal pushover analysis under a multi-component earthquake, *Technological Innovations in Nuclear Civil Engineering*, Paris, France, 2016.

[22] M. Huguet, O. Lherminier and S. Erlicher, The E-DVA pushover method for multi-modal pushover analysis with multi-component earthquake: analysis of two irregular buildings, *Technological Innovations in Nuclear Civil Engineering*, Paris-Saclay, France, 2018.

[23] www.code-aster.org/V2/doc/default/fr/man_r/r7/r7.01.08.pdf, Code_Aster.

[24] S. Erlicher, 0. Lherminier and M. Huguet, The E-DVA method: a new approach for multi-modal pushover analysis under multi-component earthquake, *Nuclear Engineering and Design*, submitted and under acceptation, 2019.

[25] ASCE-4-16, Seismic analysis of safety-related nuclear structure, *ASCE Standard*, Reston, Virginia, US, 2017.

[26] B. Richard, S. Cherubini, F. Voldoire, P.E. Charbonnel, T. Chaudat, S. Abouri, N. Bonfils, SMART 2013: Experimental and numerical assessment of the dynamic behavior by shaking table tests of an asymmetrical reinforced concrete structure subjected to high intensity ground motions, *Engineering Structures*, 109:99-116, 2016.